








Twist dependencies of strain and temperature sensitivities of perfluorinated graded-index polymer optical fiber Bragg gratings

Yosuke Mizuno^{1*} , Tianyi Ma¹, Ryo Ishikawa¹, Heeyoung Lee¹ , Antreas Theodosiou² , Kyriacos Kalli² , and Kentaro Nakamura¹ 

¹Institute of Innovative Research, Tokyo Institute of Technology, Yokohama 226-8503, Japan

²Photonics and Optical Sensing Research Laboratory, Cyprus University of Technology, Limassol 3036, Cyprus

*E-mail: ymizuno@sonic.pi.titech.ac.jp

Received May 27, 2019; revised June 17, 2019; accepted July 8, 2019; published online July 17, 2019

We measure the twist dependence of the reflected spectrum of a fiber Bragg grating (FBG) inscribed in a perfluorinated graded-index (PFGI) polymer optical fiber (POF). With increasing twist, the strain sensitivity decreases with a coefficient of -34.2 pm%/turns/m, while the temperature sensitivity increases with a coefficient of 0.39 pm/°C/turns/m. At a twist of 150 turns m^{-1} , the temperature sensitivity is 3 times higher than that with no twist. The controllability of the strain and temperature coefficients without considerable cost is beneficial not only to highly sensitive temperature sensing but also discriminative sensing of strain and temperature using two PFGI-POF-FBGs. © 2019 The Japan Society of Applied Physics

Fiber Bragg gratings (FBGs) have been widely studied for their capability of measuring various physical parameters with high precision.^{1,2)} Recently, it has become feasible to inscribe FBGs in special polymer optical fibers (POFs),^{3,4)} called perfluorinated graded-index (PFGI) POFs, which have a relatively low loss even at telecommunication wavelength.⁵⁾ PFGI-POF-FBGs have been already used to develop sensors for strain,^{6–9)} temperature,^{6,10–12)} and pressure.¹³⁾

As all the commercially available PFGI-POFs are multi-mode fibers, their FBG-reflected spectra show multiple peaks corresponding to different propagation modes.^{6–13)} One method for measuring strain etc using such multiple-peak spectra is to focus on one of the clearest peaks and track its central wavelength. This method is simple, and by exploiting multiple peaks with different dependence coefficients, discriminative sensing of multiple parameters can be potentially performed.¹¹⁾ However, the measurement stability is relatively low because of modal fluctuations. For instance, at ~ 1560 nm, the strain dependence coefficient evaluated using this method was shown to vary from 12.6 nm/% to 14.3 nm/%¹⁴⁾

To achieve stable measurement, several techniques for demodulating the Bragg wavelength from multiple-peak FBG-reflected spectra have been developed. They include centroid detection,¹⁵⁾ cross correlation,^{15,16)} Hilbert transformation,¹⁷⁾ and Lorentzian fitting.¹⁴⁾ Each algorithm has its merits and demerits, and all of these techniques have been shown to improve the measurement stability.^{14–17)} For instance, the strain coefficient calculated using the Lorentzian demodulation was almost constant at 14.1 nm/% regardless of the modal conditions.¹⁴⁾

If the strain and temperature sensitivities of a POF-FBG can be controlled without considerable cost, it is beneficial not only to highly sensitive measurement but also to discriminative sensing of strain and temperature using multiple POF-FBGs (see Refs. 18–21 for matrix-based discrimination). One candidate of the cost-effective methods for controlling the sensitivities is to apply twists to the POF-FBGs. Unlike in the case of relatively fragile silica FBGs,^{22,23)} if we exploit the high flexibility of POFs,²⁴⁾ much larger twist can be applied, which may lead to higher controllability of strain and temperature coefficients. Note

that, to the best of our knowledge, no reports have been provided as to the twist effect on PFGI-POF-FBGs.

In this study, first, we measure the twist dependence of the PFGI-POF-FBG-reflected spectrum. We find that, even when relatively large twists are applied, the Bragg wavelength does not show a clear shift, and that the spectrum is abruptly weakened at a twist of ~ 160 turns m^{-1} (still in the elastic region). Then, we measure the twist dependencies of the strain and temperature sensitivities.

An FBG was inscribed in a 1.4 m long PFGI-POF (GigaPOF-50SR, Chromis Fiberoptics)^{5,25)} using a femtosecond laser irradiation method.^{26,27)} The length of the FBG was 2 mm. The PFGI-POF had a three-layer structure involving core (diameter d : 50 μm ; refractive index n : ~ 1.35), cladding (d : 70 μm , n : ~ 1.34), and overcladding (d : 490 μm). The core and cladding were doped and undoped amorphous fluoropolymer, respectively, whereas the overcladding was polycarbonate. Its propagation loss was ~ 0.25 dB m^{-1} at 1550 nm, which is extremely low compared to that of a standard acryl-based POF.^{3,5)} Without removing the overcladding, the FBG was inscribed using a femtosecond laser system (High Q femtoREGEN, High Q Laser) at 517 nm. The pulse duration was 220 fs, the repetition rate was 1 kHz, and the pulse energy was ~ 100 nJ. The POF was fixed on an air bearing translation system for two-axis motion with high resolution and accuracy. A long-working-distance objective ($\times 50$) was mounted on the third axis, and the irradiated laser beam was focused into the POF. Plane-by-plane FBG inscription was conducted by accurately synchronizing the laser pulse repetition and the stage motion.²⁷⁾

Figure 1(a) shows the experimental setup for observing the spectrum of the light reflected from the PFGI-POF-FBG. Amplified spontaneous emission was used as a wideband light source, and the FBG-reflected spectrum was observed using an optical spectrum analyzer (AQ6370, Yokogawa; resolution: 2.0 nm). The Lorentzian demodulation method was employed to stably measure the Bragg wavelength.¹⁴⁾ As depicted in Fig. 1(b), a 100 mm long section containing the FBG at the midpoint was fixed in length, and twists were applied at one end of this section. To evaluate the strain dependence, strains were applied to the FBG by pulling the other end of this section. As for measurement of the temperature dependence, the 100 mm long section was

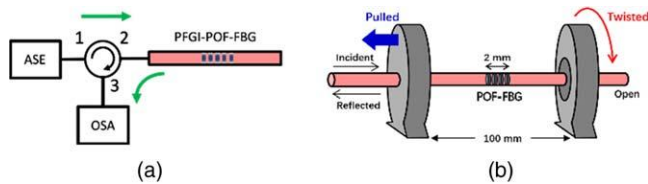


Fig. 1. (Color online) (a) Schematic of the experimental setup. ASE: amplified spontaneous emission, OSA, optical spectrum analyser. (b) Setup for applying twists to a POF-FBG.

placed on a heater (HI-1000, As One). The room temperature was 19 °C.

First, the twist dependence of the FBG-reflected spectrum was measured. Figure 2(a) shows the FBG-reflected spectra when no twist was applied and when a twist of 150 turns m^{-1} was applied. The vertical axis was normalized so that the peak power of each spectrum became 1. It is clear that the Bragg wavelength was almost the same regardless of the large twist. When the applied twist was released, the spectrum returned to the initial state with high repeatability, which indicates that the POF is still in its elastic state at a twist of 150 turns m^{-1} . Figure 2(b) shows the Bragg wavelength dependence on applied twist. No significant change in the Bragg wavelength was observed, which is natural considering that the grating pitch is not largely affected by twist because the length of the 100 mm long section was kept constant. Figure 2(c) shows the FBG-reflected spectra when

no twist was applied and when twists of 160 and 165 turns m^{-1} were applied. Here, to evaluate the twist-induced change in the peak power, the vertical axis was normalized so that the peak power of the spectrum with no twist became 1 (the proportion among the peak powers of three spectra was maintained). At ~ 160 turns m^{-1} , the spectral power started to decrease, and at 165 turns m^{-1} , the spectrum (shown without Lorentzian fitting) was buried by the noise floor. Figure 2(d) shows the dependence of the normalized spectral peak power on twist. The peak powers at >165 turns m^{-1} were defined to be 0. As the twist increased to ~ 150 turns m^{-1} , the peak power slightly increased because of the modal fluctuations, but at >160 turns m^{-1} , it was abruptly weakened. This is probably because part of the PFGI-POF started to be mechanically distorted and a considerable loss was induced there. A twist of ~ 160 turns m^{-1} should be close to the boundary of the elastic-to-plastic transition of the PFGI-POF. We confirmed that the PFGI-POF did not break even when the twist reached 800 turns m^{-1} , although the optical loss was so high that almost no light can propagate through it. As the mechanical strength of the PFGI-POF is mainly determined by the relatively thick overcladding layer composed of polycarbonate,^{28,29)} the core was probably broken at such a large twist.

Subsequently, we measured the twist dependence of the strain sensitivity. Figure 3(a) shows the measured strain

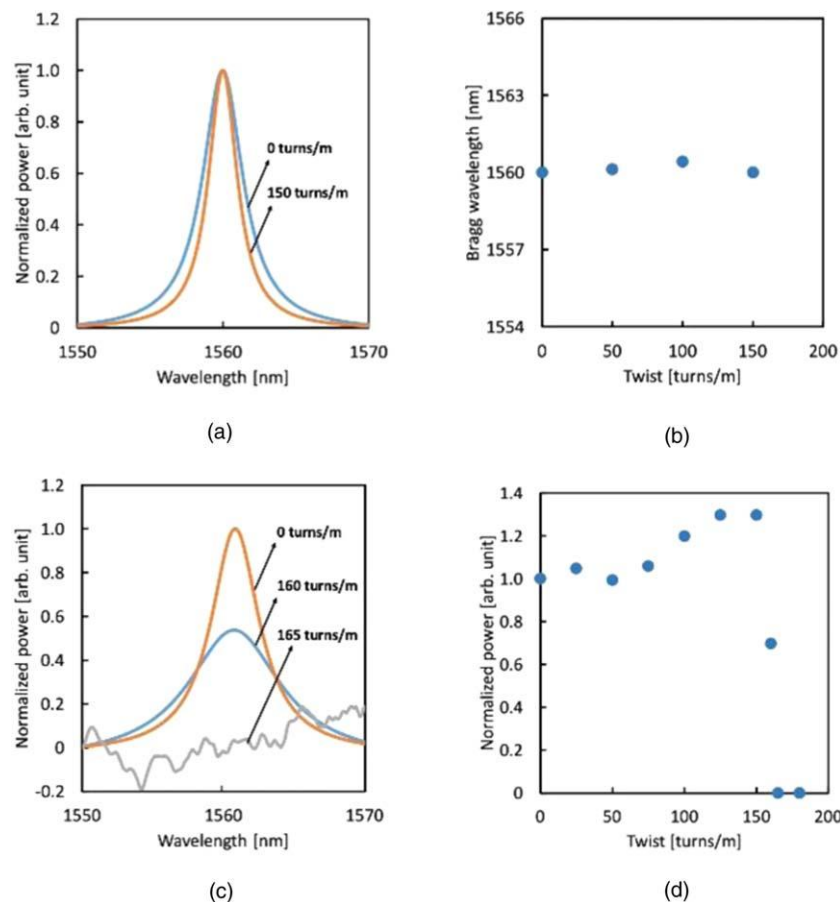


Fig. 2. (Color online) (a) FBG-reflected spectra measured when no twist was applied and when a twist of 150 turns m^{-1} was applied. The vertical axis was normalized so that the peak powers became 1. (b) Bragg wavelength dependence on twist. (c) FBG-reflected spectra measured when no twist was applied and when twists of 160 and 165 turns m^{-1} were applied. The vertical axis was normalized using the spectrum with no twist. Lorentzian fitting was not performed for the data at 165 turns m^{-1} . (d) Normalized peak power dependence on twist.

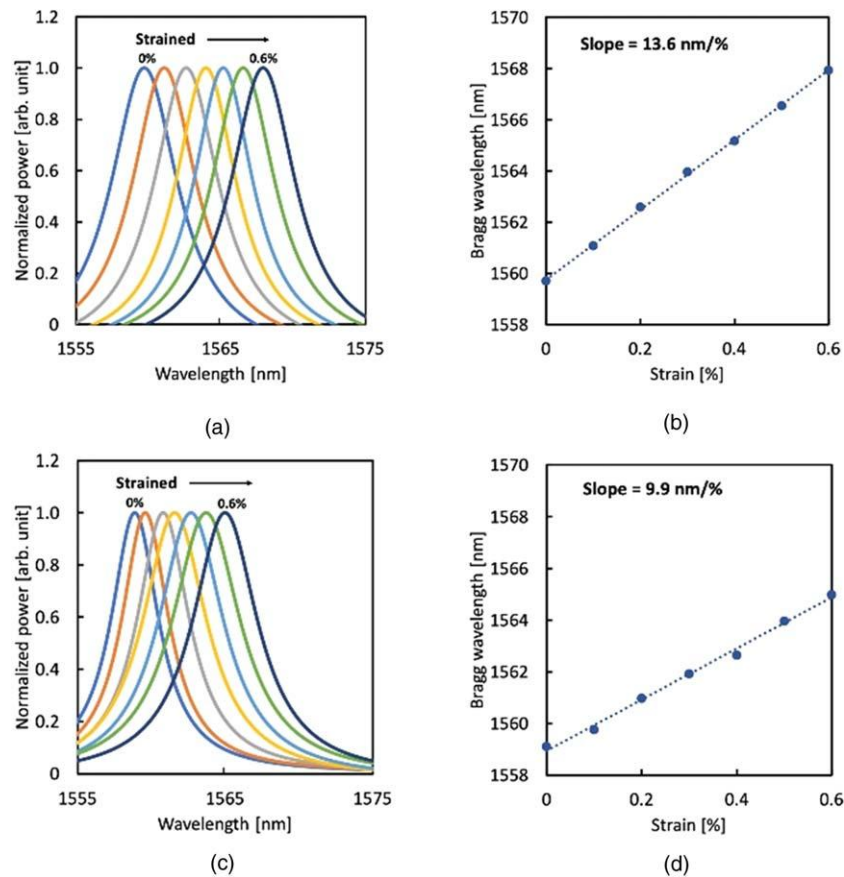


Fig. 3. (Color online) (a) Strain dependence of the FBG-reflected spectrum when no twist was applied. Step: 0.1%. (b) Bragg wavelength dependence on strain when no twist was applied. (c) Strain dependence of the FBG-reflected spectrum when a twist of 100 turns m^{-1} was applied. Step: 0.1%. (d) Bragg wavelength dependence on strain when a twist of 100 turns m^{-1} was applied. The dotted lines in (b) and (d) are linear fits.

dependence of the FBG-reflected spectrum when twist was not applied. With increasing strain, the spectrum shifted to longer wavelength. Figure 3(b) shows the strain dependence of the Bragg wavelength, which was almost linear with a coefficient of 13.6 nm/%. This value is in good agreement with the previous report.¹⁴⁾ Then, we performed the same measurements when twists were applied. The strain dependence of the FBG-reflected spectrum at a twist of 100 turns m^{-1} is shown in Fig. 3(c). As strain increased, the spectrum also shifted to longer wavelength, but the amount of the shift was smaller than at zero twist. The strain dependence of the Bragg wavelength [Fig. 3(d)] revealed that the strain coefficient was reduced to 9.9 nm/%. In the same manner, we measured the strain coefficients at other twists (50 and 150 turns m^{-1}) and plotted them as a function of twist (Fig. 4). The strain sensitivity was found to decrease with increasing twist in this twist range, and the dependence coefficient that was roughly calculated from its linear fitting was -34.2 pm/%/turns/m. This is probably because the strain dependence coefficient of the refractive index of the core was reduced by twist.

Finally, we measured the twist dependence of the temperature sensitivity. Figure 5(a) shows the measured temperature dependence of the FBG-reflected spectrum when no twist was applied. As the POF-FBG was heated, the spectrum shifted to shorter wavelength. Figure 5(b) shows the temperature dependence of the Bragg wavelength, which was almost linear with a coefficient of -30.0 pm/ $^{\circ}$ C. Although this value does not agree with the previous reports,^{6,10–12)} considering that the

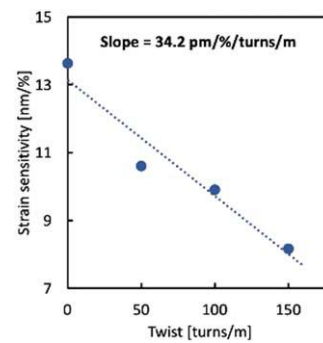


Fig. 4. (Color online) Strain sensitivity plotted as a function of twist. The dotted line is a linear fit.

measurement of the temperature dependence of the Bragg wavelength is susceptible to modal fluctuations and thus is unstable compared to that of the strain dependence,^{6,11)} this result is reasonable. Then, we applied twists and performed the same measurements. The temperature dependence of the FBG-reflected spectrum at a twist of 150 turns m^{-1} is shown in Fig. 5(c). With increasing temperature, the spectrum also shifted to shorter wavelength, but the amount of the shift was larger. The spectral bandwidth became narrower because of the modal fluctuations. Figure 5(d) shows the temperature dependence of the Bragg wavelength. Although the linearity was not high, by linear fitting, the temperature coefficient was roughly calculated to be -91.1 pm/ $^{\circ}$ C. Figure 6 shows the dependence of the temperature sensitivity (i.e., absolute value of the temperature coefficient of the Bragg wavelength) on applied

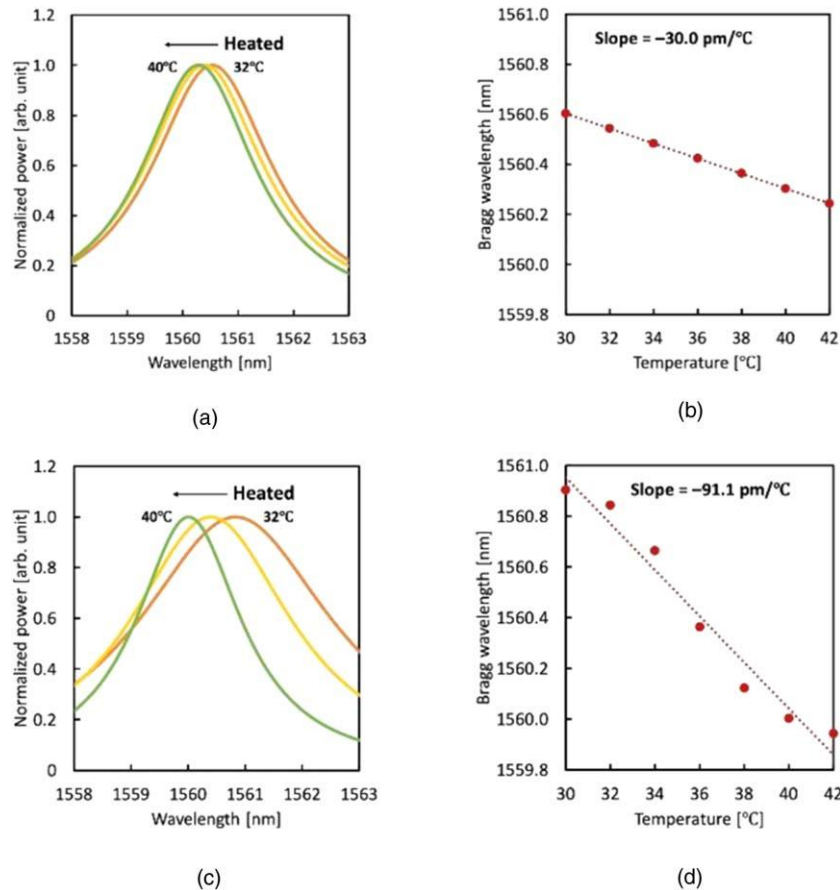


Fig. 5. (Color online) (a) Temperature dependence of the FBG-reflected spectrum when no twist was applied. Step: 4°C . (b) Bragg wavelength dependence on temperature when no twist was applied. (c) Temperature dependence of the FBG-reflected spectrum when a twist of 150 turns m^{-1} was applied. Step: 4°C . (d) Bragg wavelength dependence on temperature when a twist of 150 turns m^{-1} was applied. The dotted lines in (b) and (d) are linear fits.

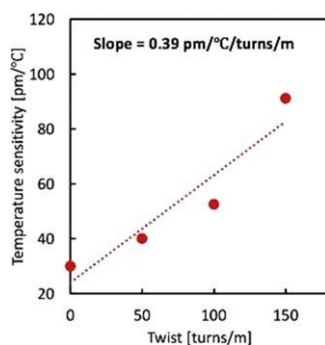


Fig. 6. (Color online) Temperature sensitivity (i.e., absolute value of the temperature coefficient of the Bragg wavelength) plotted as a function of twist. The dotted line is a linear fit.

twist. As twist increased, the temperature sensitivity increased in this twist range. Although the dependence exhibited a nonlinear increase, it was linearly fitted to roughly evaluate the dependence coefficient, which was found to be approximately $0.39 \text{ pm}/^\circ\text{C}/\text{turns/m}$. By applying a twist of 150 turns m^{-1} , the temperature sensitivity can be ~ 3 times higher than that with no twist. This behavior could be explained by assuming that the absolute value of the negative coefficient of the refractive index dependence on temperature increased by twist in this measurement.

Thus, the strain and temperature sensitivities of the PFGI-POF-FBG were experimentally proved to be controllable by twist. To apply twist to fibers involving FBGs is a cost-efficient

way to change the FBG properties and is compatible with flexible POFs, to which relatively large amount of twist can be applied. One indication of our results is that, by twisting the PFGI-POF-FBG, highly sensitive temperature sensing with reduced strain sensitivity can be performed. Another indication is that discriminative sensing of strain and temperature using non-twisted and twisted PFGI-POF-FBGs will be feasible by use of a matrix-based method.^{18–21)}

In conclusion, we measured the twist dependencies of the PFGI-POF-FBG-reflected spectrum and its strain and temperature sensitivities. Clear twist dependence of the Bragg wavelength was not observed, and at a twist of $>160 \text{ turns m}^{-1}$, the spectral peak power was abruptly reduced. With increasing twist, the strain sensitivity of the Bragg wavelength decreased with a coefficient of approximately $-34.2 \text{ pm}/\%/ \text{turns/m}$, while the temperature sensitivity increased with a coefficient of approximately $0.39 \text{ pm}/^\circ\text{C}/\text{turns/m}$. The latter indicates that, for instance, the temperature sensitivity can be enhanced ~ 3 times by applying a twist of 150 turns m^{-1} . These findings will lead to the potential feasibility not only of highly sensitive temperature sensing with lower strain sensitivity but also of discriminative sensing of strain and temperature using two PFGI-POF-FBGs. We believe that this paper will provide a useful tool for a number of researchers in the FBG sensing community.

Acknowledgments This work was supported by JSPS KAKENHI Grant Numbers 17H04930 and 17J07226 and by a research grant from the Fujikura Foundation.

ORCID iDs Yosuke Mizuno  <https://orcid.org/0000-0002-3362-4720>
 Heeyoung Lee  <https://orcid.org/0000-0003-3179-0386>
 Antreas Theodosiou  <https://orcid.org/0000-0002-5912-9138>
 Kyriacos Kalli  <https://orcid.org/0000-0003-4541-092X>
 Kentaro Nakamura  <https://orcid.org/0000-0003-2899-4484>

- 1) R. Kashyap, *Fiber Bragg Gratings* (Elsevier, San Diego, 1999).
- 2) A. Othonos and K. Kalli, *Fiber Bragg Gratings: Fundamentals and Applications in Telecommunications and Sensing* (Artech House, Boston, 1996).
- 3) M. G. Kuzyk, *Polymer Fiber Optics: Materials, Physics, and Applications* (CRC Press, San Diego, 2006).
- 4) D. J. Webb, *Meas. Sci. Technol.* **26**, 092004 (2015).
- 5) Y. Koike and M. Asai, *NPG Asia Mater.* **1**, 22 (2009).
- 6) A. Lacraz, M. Polis, A. Theodosiou, C. Koutsides, and K. Kalli, *IEEE Photonics Technol. Lett.* **27**, 693 (2015).
- 7) P. Stajanca, A. Lacraz, K. Kalli, M. Schukar, and K. Kreller, *Proc. SPIE* **9899**, 989911 (2016).
- 8) A. Leal-Junior, A. Theodosiou, C. Díaz, C. Marques, M. J. Pontes, K. Kalli, and A. Frizera, *J. Lightwave Technol.* **37**, 971 (2019).
- 9) R. Ishikawa, H. Lee, A. Lacraz, A. Theodosiou, K. Kalli, Y. Mizuno, and K. Nakamura, *Jpn. J. Appl. Phys.* **57**, 038002 (2018).
- 10) Y. Zheng, K. Bremer, and B. Roth, *Sensors* **18**, 1436 (2018).
- 11) Y. Mizuno, R. Ishikawa, H. Lee, A. Theodosiou, K. Kalli, and K. Nakamura, *IEEE Sens. J.* **19**, 4458 (2019).
- 12) M. Koerdt, S. Kibben, O. Bendig, S. Chandrashekar, J. Hesselbach, C. Brauner, A. S. Herrmann, F. Vollertsen, and L. Kroll, *Mechatron* **34**, 137 (2016).
- 13) R. Ishikawa, H. Lee, A. Lacraz, A. Theodosiou, K. Kalli, Y. Mizuno, and K. Nakamura, *IEEE Photonics Technol. Lett.* **29**, 2167 (2017).
- 14) Y. Mizuno, T. Ma, R. Ishikawa, H. Lee, A. Theodosiou, K. Kalli, and K. Nakamura, *Jpn. J. Appl. Phys.* **58**, 028003 (2019).
- 15) A. Lamberti, S. Vanlanduit, B. D. Pauw, and F. Berghmans, *Sensors* **14**, 24258 (2014).
- 16) C. Huang, W. Jing, K. Liu, Y. Zhang, and G. D. Peng, *IEEE Photonics Technol. Lett.* **19**, 707 (2007).
- 17) A. Theodosiou, M. Komodromos, and K. Kalli, *J. Lightwave Technol.* **35**, 3956 (2017).
- 18) M. Ding, Y. Mizuno, and K. Nakamura, *Opt. Express* **22**, 24706 (2014).
- 19) C. C. Lee, P. W. Chiang, and S. Chi, *IEEE Photon. Technol. Lett.* **13**, 1094 (2001).
- 20) T. R. Parker, M. Farhadiroushan, V. A. Handerek, and A. J. Rogers, *Opt. Lett.* **22**, 787 (1997).
- 21) W. Zou, Z. He, and K. Hotate, *Opt. Express* **17**, 1248 (2009).
- 22) Y. J. Rao, T. Zhu, and Q. J. Mo, *Opt. Commun.* **266**, 187 (2006).
- 23) W. Yiping, M. Wang, and X. Huang, *Opt. Express* **21**, 11913 (2013).
- 24) H. Ujihara, N. Hayashi, Y. Mizuno, and K. Nakamura, *IEICE Electron. Express* **11**, 20140707 (2014).
- 25) Y. Mizuno and K. Nakamura, *Appl. Phys. Lett.* **97**, 021103 (2010).
- 26) A. Theodosiou, A. Lacraz, M. Polis, K. Kalli, M. Tsangari, A. Stassis, and M. Komodromos, *IEEE Photonics Technol. Lett.* **28**, 1509 (2016).
- 27) A. Theodosiou, A. Lacraz, A. Stassis, C. Koutsides, M. Komodromos, and K. Kalli, *J. Lightwave Technol.* **35**, 5404 (2017).
- 28) N. Hayashi, K. Minakawa, Y. Mizuno, and K. Nakamura, *Appl. Phys. Lett.* **105**, 091113 (2014).
- 29) Y. Mizuno, N. Matsutani, N. Hayashi, H. Lee, M. Tahara, H. Hosoda, and K. Nakamura, *Opt. Express* **26**, 28030 (2018).